24 October 1997

ELSEVIER

Chemical Physics Letters 278 (1997) 175–183

CHEMICAL PHYSICS LETTERS

Sensitivity of two-dimensional fifth-order Raman response to the mechanism of vibrational mode–mode coupling in liquid molecules

K. Okumura, Y. Tanimura

Division of Theoretical Studies, Institute for Molecular Science, Myodaiji, Okazaki, Aichi 444, Japan

Received 22 July 1997; in final form 6 August 1997

Abstract

We study coupling mechanism of inter- and intramolecular modes of liquids by using a multi-mode Brownian oscillators model. The coupling between modes comes into play through polarizability and/or potential expanded with respect to vibrational coordinates. We take into account these two causes of coupling and present analytical expressions for the Fourier transform of the time-domain fifth-order Raman signal. We demonstrate a notable sensitivity of the Fourier-transformed quantity to the coupling mechanism through numerical calculations for chloroform. © 1997 Elsevier Science B.V.

1. Introduction

The fifth-order off-resonant spectroscopy has received considerable attention since the initial proposal [1], because this two-dimensional (2D) Raman spectroscopy has the potential to probe inhomogeneous dynamics in the condensed phase. Experimental [2–11] and theoretical [12–18] studies have been made to explore the possibility to detect such heterogeneity. Until recently the experimental investigation had been limited to the cases of the low frequency intermolecular vibrational modes of liquid molecules such as CS_2 since they could not use pulses short enough to probe faster intramolecular vibrational dynamics in order to detect the weak fifth-order signal. A novel heterodyne detection of 2D Raman spectroscopy has now become possible where shorter pulses can be used to probe the intramolecular dynamics [10,11].

To interpret the response due to such higher frequency modes, the 2D Fourier transform of the time-domain 2D Raman signal is useful. The Fourier-transformed results from the time-domain experiments have indicated a sign of the coupling between inter- and/or intramolecular modes in CS_2, CCl_4 and $CHCl_3$ liquids [10,11]. In the mixture of CCl_4 and $CHCl_3$, the couplings between a mode of CCl_4 and that of $CHCl_3$ have been suggested [11]. These results show that the Fourier-transformed results could be used to investigate the coupling mechanism.

PII S0009-2614(97)00942-1

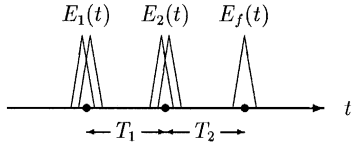

Fig. 1. Pulse sequence and time variables for the fifth-order Raman experiment. The first femtosecond pulse pair excites Raman modes, the second pulse pair after the delay time T_1 causes further Raman interactions, and the final probe pulse after the delay T_2 induces the signal.

The quantity observed in the time-domain experiment is a three-time response function [19] of the polarizability α which can be expressed as

$$R^{(5)}(T_1,T_2) = \left(\frac{i}{\hbar}\right)^2 \langle [[\alpha(T_1+T_2),\alpha(T_2)],\alpha(0)]\rangle, \tag{1.1}$$

where T_1 and T_2 refer to the time intervals between pulses (see Fig. 1). It has been shown that, in order to have a nonzero signal, one has to assume either nonlinear dependence of polarizability [e.g., $\alpha(Q) = \alpha_1 Q + \alpha_2 Q^2$ for a single mode Q] or anharmonicity in the vibrational potential [e.g., $V(Q) = gQ^3$] [20]. Accordingly, modes can couple with each other through two types of mechanism: polarizability-induced coupling and anharmonic coupling. The former is the coupling between modes through nonlinearity of α (e.g., the cross term Q_1Q_2 in the expansion of α where Q_1,Q_2 are the vibrational coordinates). The latter is the one through anharmonic coupling in the vibrational potential $V(Q)$ [e.g., the anharmonic term $Q_1Q_2^2$ in the expansion of $V(Q)$]. (See Section 2 for detail.)

In this paper we present analytical expressions for the fifth-order time-domain response and its Fourier transform with the two types of coupling mechanism taken into account. From the expressions, we predict the positions of peaks for weak damping modes and explicitly show that cross peaks cannot appear in the mode-decoupled case: they originate from either polarizability-induced or anharmonic coupling. To demonstrate a possibility to investigate the relative importance of the two mechanisms, we perform numerical simulations for chloroform by using parameters extracted from the third-order experiment, and compare them with the experimental data obtained by Tokmakoff et al. [11]. The result shows a distinct sensitivity of the 2D Raman response to coupling mechanism and gives some microscopic information on the mode–mode coupling.

2. Model and analytical expressions for the 2D response

We consider the effective Hamiltonian of a molecular system irradiated with pairs of off-resonant pulses which is given by

$$H = H_{\rm V} + H_{\rm VL} + H_{\rm B}, \tag{2.1}$$

where $H_{\rm V}$, $H_{\rm VL}$, and $H_{\rm B}$ are, respectively, the Hamiltonian of the molecular vibrational motion, the laser interaction, and the heat bath.

The Hamiltonian, $H_{\rm V}$, is described by n oscillators with frequency Ω_s's;

$$H_{\rm V} = \sum_{s=1}^{n}\left(\frac{P_s^2}{2M_s} + \frac{M_s\Omega_s^2}{2}Q_s^2\right) + V(Q). \tag{2.2}$$

Here, Q collectively denotes the coordinates $Q_1,Q_2,\ldots$. The oscillators are mutually coupled through the anharmonic potential,

$$V(Q) = \sum_{s,s',s''}\frac{g_{ss's''}}{3!}Q_sQ_{s'}Q_{s''} + \cdots, \tag{2.3}$$

where $g_{ss's''} \equiv \partial^3 V(Q)/\partial Q_s\partial Q_{s'}\partial Q_{s''}$ is the coupling parameter and "$\cdots$" denotes the higher-order expansion terms. Note that this third-order coupling $Q_sQ_{s'}Q_{s''}$ is the simplest but nontrivial one (the Q_1Q_2 term, for example, is trivial since it can be removed by changing the set of normal modes).

The vibrational motion and the off-resonant pulses are coupled through the coordinate-dependent polarizability $\alpha(Q)$;

$$H_{\rm VL} = -\alpha(Q)\,E(\boldsymbol{r},t)^2, \tag{2.4}$$

where we have employed the semiclassical approximation in which the electronic field $E(\boldsymbol{r},t)$ is treated as c-number while the polarizability $\alpha(Q)$ is a quantum-operator. The polarizability is generally expanded as

$$\alpha(Q) = \alpha_0 + \sum_s \alpha_1^{(s)} Q_s + \sum_{s,s'} \frac{\alpha_2^{(ss')}}{2!} Q_s Q_{s'} + \cdots, \tag{2.5}$$

where α_0, $\alpha_1^{(s)} \equiv \partial\alpha(Q)/\partial Q_s$, and $\alpha_2^{(ss')} \equiv \partial^2\alpha(Q)/\partial Q_s \partial Q_{s'}$ are parameters. Thus, $\alpha(Q)$ involves cross terms such as $\alpha_2^{(12)} Q_1 Q_2$.

We take into account the effects of dissipation on vibrational modes by the harmonic heat bath Hamiltonian,

$$H_{\rm B} = \sum_{s=1}^{n} \sum_{i=1}^{N} \left[\frac{p_{s,i}^2}{2m_{s,i}} + \frac{m_{s,i}\omega_{s,i}^2}{2} \left(q_{s,i} - \frac{c_{s,i} Q_s}{m_{s,i}\omega_{s,i}} \right)^2 \right], \tag{2.6}$$

where the conventional notation is employed. In the following we assume the Ohmic dissipation in which all the bath parameters $(m_{s,i}, \omega_{s,i}, c_{s,i})$ for the sth mode are represented by the single parameter γ_s. This γ_s can be interpreted as the strength of damping of the sth vibrational mode [21,22].

Under the assumption that the anharmonicity, $V(Q)$, and the nonlinear polarizability, $\alpha(Q) - \alpha_0 - \sum_s \alpha_1^{(s)} Q_s$, are weak (see Ref. [20] for detail), the time-domain fifth-order response is given by

$$R^{(5)}(T_1,T_2) = R_{\rm P} + R_{\rm A}, \tag{2.7}$$

where the polarizability-induced term $R_{\rm P}$ is the contribution proportional to $\alpha_1^{(s)}\alpha_1^{(s)}\alpha_2^{(ss')}$, which vanishes if the polarizability is assumed to be linear (i.e., $\alpha(Q) = \alpha_0 + \sum_s \alpha_1^{(s)} Q_s$), and the anharmonic term $R_{\rm A}$ is the one proportional to $g_{ss's''}$, which vanishes if the anharmonic coupling $V(Q)$ is neglected. In Section 3, we consider two limiting cases for a demonstration: the polarizability-induced coupling case where the fifth-order response is given by $R^{(5)}(T_1,T_2) = R_{\rm P}$ and the anharmonic coupling case where $R^{(5)}(T_1,T_2) = R_{\rm A}$. The actual profile of Eq. (2.7) should be determined by the contribution from both terms.

The polarizability-induced term $R_{\rm P}$ had already been derived in Refs. [1,20] under the assumption of the exponential polarizability where $\alpha_2^{(ss')}/\alpha_0 = (\alpha_1^{(s)}/\alpha_0)(\alpha_1^{(s')}/\alpha_0)$. The extension to a general case in Eq. (2.5) can be done by using the Feynman rule on the unified time-path [20,22–26]. The result is

$$R_{\rm P} = \left(\frac{i}{\hbar}\right)^2 \sum_{ss'} \alpha_1^{(s)}\alpha_1^{(s')}\alpha_2^{(ss')} D_s^{(-+)}(T_2) \left[D_{s'}^{(-+)}(T_1+T_2) + D_{s'}^{(-+)}(T_1) \right], \tag{2.8}$$

where the propagator $D_s^{(-+)}(t)$ is defined by

$$D_s^{(-+)}(t) = \theta(t) \frac{\hbar}{iM_s\zeta_s} \mathrm{e}^{-\gamma_s t/2} \sin\zeta_s t, \tag{2.9}$$

where $\theta(t)$ is the Heaviside's step function and the frequency ζ_s is given by

$$\zeta_s \equiv \sqrt{\Omega_s^2 - \gamma_s^2/4}\,. \tag{2.10}$$

It should be noted here that the frequency ζ_s can take an imaginary value for the overdamped mode where $\Omega_s < \gamma_s/2$. The derivation of Eq. (2.8) is parallel to that in Ref. [20] and we only note that Eq. (2.8) reduces to Eq. (C4) of Ref. [20] under the exponential assumption $\alpha_2^{(ss')}/\alpha_0 = (\alpha_1^{(s)}/\alpha_0)(\alpha_1^{(s')}/\alpha_0)$.

The anharmonic term $R_{\rm A}$ can be also derived by using the Feynman rule on the unified time-path and the result is

$$R_{\rm A} = \sum_{ss's''} g_{ss's''} R_{ss's''}, \tag{2.11}$$

where

$$R_{ss's''} = -\left(\frac{i}{\hbar}\right)^3 \alpha_1^{(s)}\alpha_1^{(s')}\alpha_1^{(s'')}\int_0^\infty {\rm d}t\, D_s^{(-+)}(T_1+T_2-t)\, D_{s'}^{(-+)}(t)\, D_{s''}^{(-+)}(t-T_1). \tag{2.12}$$

(The derivation is again parallel to that in Ref. [20]. We note here that $R_{ss's''}$ reduces to (C3) of Ref. [20] when $s=s'=s''$. Namely, the response of the single mode with the cubic anharmonicity Q_s^3 is given by R_{sss}.)

Although the above results are obtained through the Feynman rule on the unified time path, which includes temperature effects, the expressions (2.8) and (2.11) do not depend on the temperature. This is because these observables have a weak temperature dependence which can be safely neglected under the assumption of weak expansion parameters. Temperature effects come into play in higher order corrections for the expansion parameters such as $g_{ss's''}$, $\alpha_1^{(s)}$, and $\alpha_2^{(ss')}$, which can be confirmed by writing down the Feynman diagrams on the unified time path [20].

The plots presented in Refs. [10,11] are the absolute value of the 2D Fourier transform of the time-domain 2D Raman response defined by

$$\tilde{R}^{(5)}(\omega_1,\omega_2) = \int_0^\infty {\rm d}T_1 \int_0^\infty {\rm d}T_2\, {\rm e}^{i\omega_1 T_1}\, {\rm e}^{i\omega_2 T_2}\, R^{(5)}(T_1,T_2). \tag{2.13}$$

By calculation parallel to that in Appendix B of Ref. [20], we obtain convenient time-domain expressions in Eqs. (A.1) and (B.1). From these expressions we get the analytical expression for the Fourier-transformed response,

$$\tilde{R}^{(5)}(\omega_1,\omega_2) = \tilde{R}_{\rm P} + \tilde{R}_{\rm A}. \tag{2.14}$$

The polarizability-induced term, $\tilde{R}_{\rm P}$, is calculated as

$$\tilde{R}_{\rm P} = \frac{\alpha_0^3}{2\hbar^2}\sum_{ss'}\frac{\tilde{\alpha}_1^{(s)}\tilde{\alpha}_1^{(s')}\tilde{\alpha}_2^{(ss')}}{\tilde{\zeta}_s\tilde{\zeta}_{s'}}\sum_{n=1}^{4}(-1)^n\frac{-\Omega_{1n}\Omega_{2n}+\Gamma\Gamma_n - i\Gamma_n\omega_1 - i\Gamma\omega_2 - \omega_1\omega_2}{\left(\Gamma^2+\Omega_{1n}^2-2i\Gamma\omega_1-\omega_1^2\right)\left(\Gamma_n^2+\Omega_{2n}^2-2i\Gamma_n\omega_2-\omega_2^2\right)}, \tag{2.15}$$

where the dimensionless parameters $\tilde{\alpha}_1^{(s)}$, $\tilde{\alpha}_2^{(ss')}$, and $\tilde{\zeta}_s$ are defined by

$$\tilde{\alpha}_1^{(s)} \equiv \frac{\alpha_1^{(s)}}{\alpha_0}\sqrt{\frac{\hbar}{M_s\Omega_0}}, \quad \tilde{\alpha}_2^{(ss')} \equiv \frac{\alpha_2^{(ss')}}{\alpha_0}\sqrt{\frac{\hbar^2}{M_sM_{s'}\Omega_0^2}}, \tag{2.16}$$

and

$$\tilde{\zeta}_s = \zeta_s/\Omega_0, \tag{2.17}$$

where Ω_0 is the unit of frequency which can be any value. The *peak frequencies* $(\Omega_{1n},\Omega_{2n})$ and the *peak widths* (Γ,Γ_n) are, respectively, linear combinations of $(\gamma_s,\gamma_{s'})$ and $(\zeta_s,\zeta_{s'})$ as explicitly given in Appendix A. As seen from Eq. (2.15), peaks appear around at $(\omega_1,\omega_2)=(\pm\Omega_i,\pm\Omega_j),(\pm\Omega_i,\pm\Omega_i\pm\Omega_j)$ for a weak damping case [In Eq. (A.2), $\zeta_s=\sqrt{\Omega_s^2-\gamma_s^2/4}\sim\Omega_s$ when γ_s is small]. This implies that, in addition to the diagonal and overtone peaks $(i=j)$, we have cross peaks $(i\neq j)$. The reason only ω_2 can be combination frequencies $(\omega_2=\pm\Omega_i\pm\Omega_j)$ shall be explained in Section 3.

The anharmonic term, $\tilde{R}_{\mathrm{A}}$, is given by

$$\tilde{R}_{\mathrm{A}} = \sum_{ss's''} \tilde{g}_{ss's''} \tilde{R}_{ss's''}, \tag{2.18}$$

where

$$\tilde{R}_{ss's''} = -\frac{\alpha_0^3 \Omega_0 \tilde{\alpha}_1^{(s)} \tilde{\alpha}_1^{(s')} \tilde{\alpha}_1^{(s'')}}{4\hbar^2 \tilde{\zeta}_s \tilde{\zeta}_{s'} \tilde{\zeta}_{s''}} \sum_{n=1}^{4} (-1)^n \left(\tilde{F}_{1n} - \tilde{F}_{2n} \right), \tag{2.19}$$

with the dimensionless parameter $\tilde{g}_{ss's''}$ defined by

$$\tilde{g}_{ss's''} \equiv \frac{g_{ss's''}}{\hbar \Omega_0} \left(\frac{\hbar^3}{M_s M_{s'} M_{s''} \Omega_0^3} \right)^{1/2}. \tag{2.20}$$

In the above we have introduced the auxiliary function $\tilde{F}_{mn}$ given by

$$\tilde{F}_{mn} = \frac{\Gamma_0 \left[\Omega_{2n}^{(m)} (\Gamma - i\omega_1) + \Omega_{1n} (\Gamma_m - i\omega_2) \right] + \Omega_{0n} \left(-\Omega_{1n} \Omega_{2n}^{(m)} + \Gamma\Gamma_m - i\Gamma_m \omega_1 - i\Gamma\omega_2 - \omega_1\omega_2 \right)}{\left(\Gamma_0^2 + \Omega_{0n}^2 \right) \left(\Gamma^2 + \Omega_{1n}^2 - 2i\Gamma\omega_1 - \omega_1^2 \right) \left[\Gamma_m^2 + \left(\Omega_{2n}^{(m)} \right)^2 - 2i\Gamma_m \omega_2 - \omega_2^2 \right]}, \tag{2.21}$$

where the peak frequencies $(\Omega_{0n}, \Omega_{1n}, \Omega_{2n}^{(m)})$ and the peak widths $(\Gamma_0, \Gamma, \Gamma_m)$ are, respectively, linear combinations of $(\gamma_s, \gamma_{s'}, \gamma_{s''})$ and $(\zeta_s, \zeta_{s'}, \zeta_{s''})$ as given in Appendix B. From Eqs. (2.19) and (2.21), we expect to have peaks around at $(\omega_1, \omega_2) = (\pm\Omega_i, \pm\Omega_j), (\pm\Omega_i, \pm\Omega_i \pm \Omega_j)$ for a weak damping case [as in the polarizability induced term, Eq. (2.15)].

As mentioned before, the time-domain counterparts of the above expressions (2.15) and (2.19) are given in Appendices A and B [Eqs. (A.1) and (B.1)]. The expression of the time-domain anharmonic term, Eq. (B.1), is more convenient for the numerical simulations than Eq. (2.12) since it does not involve the time integration.

Finally we consider the case in which $V(Q) = 0$ and $\alpha(Q) = \alpha_0 + \sum_s (\alpha_1^{(s)} Q_s + \alpha_2^{(ss)} Q_s^2/2 + \cdots)$. This case shall be called mode-decoupled case since there is no coupling between different modes. [Notice that there are no cross terms such as $Q_1 Q_2$ in this form of polarizability $\alpha(Q)$.] In this case the response can be expressed by a simple summation of the contribution from each mode as

$$R^{(5)}(T_1, T_2) = \left(\frac{i}{\hbar} \right)^2 \sum_s \left(\alpha_1^{(s)} \right)^2 \alpha_2^{(ss)} D_s^{(-+)}(T_2) \left[D_s^{(-+)}(T_1 + T_2) + D_s^{(-+)}(T_1) \right]. \tag{2.22}$$

The Fourier transformation of the response (2.22) is obtained from Eq. (2.15) by inserting the Kronecker's delta $\delta_{ss'}$ after the summation symbol with respect to s and s'. From this expression, we see that the peaks appear only around at $(\omega_1, \omega_2) = (\pm\Omega_i, \pm\Omega_i), (\pm\Omega_i, \pm 2\Omega_i), (\pm\Omega_i, 0)$ for a weak damping case. This means that any cross peaks cannot appear in the mode-decoupled case.

3. Comparison with the experimental data

To demonstrate how coupling mechanisms affect on the 2D signal, we perform numerical simulations and compare them with experimental data. Here, we consider chloroform whose low frequency (Raman active) vibrational response is characterized by three modes. From the third-order off-resonant experiment [27], we can extract the following parameters almost uniquely [20]:

$$\begin{pmatrix} \Omega_1 & \gamma_1 & \eta_1 \\ \Omega_2 & \gamma_2 & \eta_2 \\ \Omega_3 & \gamma_3 & \eta_3 \end{pmatrix} = \begin{pmatrix} 39.0 & 77.0 & 1.17 \\ 258.5 & 15.0 & 2.10 \\ 368.5 & 22.0 & 1.25 \end{pmatrix} \tag{3.1}$$

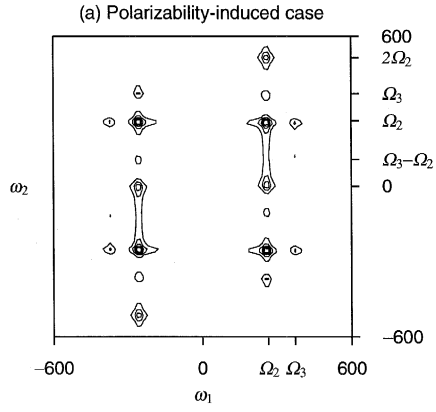

Fig. 2. Contour plot of the absolute value, $|\tilde{R}(\omega_1,\omega_2)|$, in (a) the polarizability-induced case. The two intramolecular modes Ω_2 and Ω_3 and their differences are shown in this figure.

where the unit is [cm^{-1}]. Here, $\eta_s = \left(\tilde{\alpha}_1^{(s)}\right)^2 \Omega_s$. The lowest mode Ω_1 can be ascribed to an intermolecular one while the other modes can be assigned to intramolecular modes.

In Ref. [11], the absolute value of Fourier-transformed response, $|\tilde{R}^{(5)}(\omega_1,\omega_2)|$, of $CHCl_3$ is plotted in the frequency range $\omega_1 = -600 \sim 600$[cm^{-1}] and $\omega_2 = 0 \sim 600$[cm^{-1}]. In the plot range, in addition to diagonal peaks positioned at $(\omega_1,\omega_2) = (\pm\Omega_i, \pm\Omega_i)$, we observe a few cross peaks. As mentioned in Section 2, these cross peaks cannot be obtained from the mode-decoupled model and carry an important information on the mode coupling mechanism.

We describe this substance by the mode-coupling model employed in the previous section: we consider the two intramolecular modes Ω_2 and Ω_3 and analyze the coupling mechanism between these two modes. (Inclusion of the lowest mode Ω_1 is discussed in Section 4.) We consider three cases of coupling: (a) polarizability-induced case, (b) intrinsic case 1, and (c) intrinsic case 2. In (a) we assume that the polarizability has the exponential form ($\tilde{\alpha}_2^{(ss')} = \tilde{\alpha}_1^{(s)}\tilde{\alpha}_1^{(s')}$) and the anharmonicity is zero [$V(Q) = 0$] so that origin of the all cross peaks is attributed to the polarizability. In (b) or (c) we assume that the polarizability is linear (i.e., $\alpha(Q) = \alpha_0 + \sum_s \alpha_1^{(s)} Q_s$) and $g_{ss's''}$ is zero except that $g_{233} = g_{323} = g_{332} = g$ or $g_{322} = g_{232} = g_{223} = g$ so that the source of the cross peaks is the intrinsic coupling $V(Q) = gQ_2Q_3^2/2$ or $gQ_3Q_2^2/2$. Here, g can be any value in our simulation, since it only determines the absolute intensities but does not change the profile; g is not important unless if the mixture of the two couplings is discussed. [We do not consider the case where g_{sss} is

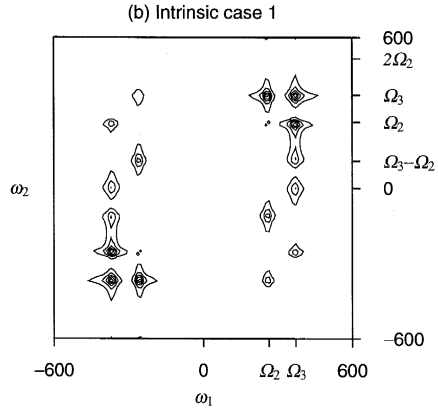

Fig. 3. Contour plot of the absolute value, $|\tilde{R}(\omega_1,\omega_2)|$, in (b) the intrinsic case 1, where $V(Q) = gQ_2Q_3^2/2$.

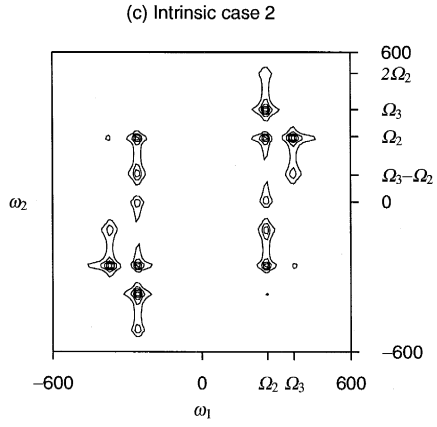

Fig. 4. Contour plot of the absolute value, $|\tilde{R}(\omega_1,\omega_2)|$, in (c) the intrinsic case 2, where $V(Q) = gQ_3Q_2^2/2$.

nonzero since this introduces the purely cubic term Q_s^3 which can not be the source for the cross peaks (but for overtone peaks) within the present approximation.]

Contour plots of the responses in the three cases (a)–(c) are presented in Figs. 2–4. These plots exhibit notable differences, suggesting a sensitivity of the 2D Raman response to coupling mechanisms. In all cases, ω_1 of the central position of each peak is one of the fundamental frequencies, that is, $\omega_1 = \pm\Omega_2$, or $\omega_1 = \pm\Omega_3$, whereas ω_2 of the central position of each peak can be a combination of the fundamental frequencies such as $\omega_2 = \Omega_3 - \Omega_2$. (The peaks along $\omega_2 = 0$ are irrelevant in the present simulations since the lowest Ω_1 mode is not taken into account – see Section 4.) This is because the time evolution after the excitation of the fundamental frequencies by the first pulse pair are being probed during the period T_1, whereas that after the excitation of combination frequencies, which is not possible until the irradiation of the second pulse pair, are being probed during T_2. We stress here that all the peaks appearing in numerical results are observed at the positions predicted from Eqs. (2.15) and (2.19) in Section 2. (However, some of the predicted peaks have a small intensities and can not be seen in the contour plots.)

By comparing these plots with the experimental result in Ref. [11], we conclude that case (b) is the closest of the three cases to the experiment. If the three cases (a)–(c) are compared, only in case (b), the peaks along $\omega_1 = \Omega_3$ and that along $\omega_1 = -\Omega_3$ are, respectively, more distinctive as a whole than the peaks along $\omega_1 = \Omega_2$ and that along $\omega_1 = -\Omega_2$. This feature of (b) is also notable in the experimental data in Ref. [11] although the result in case (b) does not perfectly fit to the experimental data. These arguments *indicates* that the coupling between the modes Q_2 and Q_3 observed in the experiment can be attributed to the $Q_2Q_3^2$ term rather than the other two terms examined here.

4. Discussion

In the present analysis of chloroform, we have not presented the numerical results where all the the three modes are included; we have performed such three-mode calculations and we have determined to show the case of two modes (Ω_2 and Ω_3) instead of three because of the following reasons. First, the inclusion of the Ω_1 mode without coupling to the other two modes merely add a peak around $(\omega_1,\omega_2) = (0,0)$. Second, when the Ω_1 mode is coupled with the other modes, new peaks appear on the ω_2 axis ($\omega_1 = 0$) and intensities of the peaks on the ω_1 axis are rather changed. However, if we subtract these peaks on the axes, the relative intensities and the profiles of the residual peaks off the axes are similar to the ones obtained here, when the coupling between Ω_1 and Ω_2 or Ω_3 is weaker than that between Ω_2 and Ω_3; this weak coupling between Ω_1 and Ω_2 or Ω_3 can be expected in the present case where $\Omega_3 - \Omega_2 < \Omega_2 - \Omega_1$. [These features have been confirmed by

numerical calculations and can be also understood from Eqs. (2.15) and (2.19).] Third, our main purpose of this paper is to demonstrate sensitivity of our expressions to the coupling mechanism rather than to make a perfect fitting; in the simpler model, discussion can be made simple and clear. Thus, we excluded the Ω_1 mode from our analysis although it is not difficult to include the Ω_1 mode in addition to the Ω_2 and Ω_3 modes.

The reproduction of the cross peaks in our simulation is reasonable but is not perfect. There is much room for improvement of our fitting, such as inclusion of higher order coupling terms, which may introduce an explicit temperature dependence. For example, the feature found in case (b) which is common to the experimental data (discussed in Section 3) might be observed even in the polarizability-induced model, if we increase the magnitude of coefficient $\alpha_2^{(33)}$ of the Q_3^2 term in the expansion of polarizability $\alpha(Q)$. We leave such improvements for a future study.

In conclusion, we present an analytical expression for the 2D Raman response with two coupling mechanisms taken into account, from which we can predict the position of peaks. Numerical estimation of the expression shows a distinct sensitivity of the signal to relative importance of the two coupling mechanisms. This clearly demonstrates that 2D Raman responses and their expressions presented in this paper can be a powerful tool in investigating the coupling mechanism. Comparison with the experimental data on chloroform gives some information on the microscopic coupling mechanism.

Acknowledgements

We would like to thank Dr. Andrei Tokmakoff for providing access to preprints and data prior to publication. The present work was supported by a Grand in Aid for Scientific Research from the Japan Ministry of Education, Science, Sports and Culture.

Appendix A. Expression for the polarizability-induced term of the time-domain 2D response

The polarizability-induced part of the fifth-order response function, R_{P}, in Eq. (2.15) can be cast into the following form (the derivation is parallel to that in Appendix B of Ref. [20]):

$$R_{\mathrm{P}} = \frac{\alpha_0^3}{2\hbar^2} \sum_{ss'} \frac{\tilde{\alpha}_1^{(s)} \tilde{\alpha}_1^{(s')} \tilde{\alpha}_2^{(ss')}}{\tilde{\zeta}_s \tilde{\zeta}_{s'}} \sum_{n=1}^{4} (-1)^n \mathrm{e}^{-\Gamma T_1 - \Gamma_n T_2} \cos(\Omega_{1n} T_1 + \Omega_{2n} T_2), \tag{A.1}$$

where

$$\Gamma = \gamma_{s'}/2, \quad \begin{pmatrix} \Gamma_1 & \Omega_{11} & \Omega_{21} \\ \Gamma_2 & \Omega_{12} & \Omega_{22} \\ \Gamma_3 & \Omega_{13} & \Omega_{23} \\ \Gamma_4 & \Omega_{14} & \Omega_{24} \end{pmatrix} = \begin{pmatrix} \gamma_s/2 & \zeta_{s'} & \zeta_s \\ \gamma_s/2 & -\zeta_{s'} & \zeta_s \\ (\gamma_s + \gamma_{s'})/2 & \zeta_{s'} & \zeta_s + \zeta_{s'} \\ (\gamma_s + \gamma_{s'})/2 & -\zeta_{s'} & \zeta_s - \zeta_{s'} \end{pmatrix}. \tag{A.2}$$

Appendix B. Expression for the anharmonic term of the time-domain 2D response

The anharmonic part of the fifth-order response function, $R_{ss's''}$, in Eq. (2.12) can be cast into the following form in the case of $T_1, T_2 > 0$ (the derivation is parallel to that in Appendix B of Ref. [20]):

$$R_{ss's''} = -\frac{\alpha_0^3 \Omega_0 \tilde{\alpha}_1^{s} \tilde{\alpha}_1^{s'} \tilde{\alpha}_1^{s''}}{4\hbar^2 \bar{g}_{ss's''} \tilde{\zeta}_s \tilde{\zeta}_{s'} \tilde{\zeta}_{s''}} \sum_{n=1}^{4} (-1)^n (F_{1n} - F_{2n}), \tag{B.1}$$

where $\bar{g}_{ss's''}$ has the dimension of the coupling parameter $g_{ss's''}$ and defined by

$$\bar{g}_{ss's''} \equiv \hbar \Omega_0 \left(\frac{M_s M'_s M''_s \Omega_0^3}{\hbar^3} \right)^{1/2} . \tag{B.2}$$

The auxiliary function F_{mn} is given by

$$F_{mn} = \frac{\mathrm{e}^{-\Gamma T_1 - \Gamma_m T_2}}{\Gamma_0^2 + \Omega_{0n}^2} \left[\Omega_{0n} \cos\left(\Omega_{1n} T_1 + \Omega_{2n}^{(m)} T_2 \right) + \Gamma_0 \sin\left(\Omega_{1n} T_1 + \Omega_{2n}^{(m)} T_2 \right) \right], \tag{B.3}$$

where

$$\begin{pmatrix} \Gamma_0 & \Gamma & \Gamma_1 & \Gamma_2 \\ \Omega_{01} & \Omega_{11} & \Omega_{21}^{(1)} & \Omega_{21}^{(2)} \\ \Omega_{02} & \Omega_{12} & \Omega_{22}^{(1)} & \Omega_{22}^{(2)} \\ \Omega_{03} & \Omega_{13} & \Omega_{23}^{(1)} & \Omega_{23}^{(2)} \\ \Omega_{04} & \Omega_{14} & \Omega_{24}^{(1)} & \Omega_{24}^{(2)} \end{pmatrix} = \begin{pmatrix} (-\gamma_s + \gamma_{s'} + \gamma_{s''})/2 & \gamma_{s'}/2 & (\gamma_{s'} + \gamma_{s''})/2 & \gamma_s/2 \\ -\zeta_s - \zeta_{s'} + \zeta_{s''} & -\zeta_{s'} & -\zeta_{s'} + \zeta_{s''} & \zeta_s \\ -\zeta_s + \zeta_{s'} + \zeta_{s''} & \zeta_{s'} & \zeta_{s'} + \zeta_{s''} & \zeta_s \\ -\zeta_s + \zeta_{s'} - \zeta_{s''} & \zeta_{s'} & \zeta_{s'} - \zeta_{s''} & \zeta_s \\ -\zeta_s - \zeta_{s'} - \zeta_{s''} & -\zeta_{s'} & -\zeta_{s'} - \zeta_{s''} & \zeta_s \end{pmatrix}. \tag{B.4}$$

References

[1] Y. Tanimura, S. Mukamel, J. Chem. Phys. 99 (1993) 9496.
[2] K. Tominaga, K. Yoshihara, Phys. Rev. Lett. 74 (1995) 3061.
[3] K. Tominaga, G.P. Keogh, Y. Naitoh, K. Yoshihara, J. Raman Spectrosc. 26 (1995) 495.
[4] K. Tominaga, K. Yoshihara, J. Chem. Phys. 104 (1996) 1159.
[5] K. Tominaga, K. Yoshihara, J. Chem. Phys. 104 (1996) 4419.
[6] K. Tominaga, Off-resonant Fifth and Seventh Order Time-Domain Nonlinear Spectroscopy on Vibrational Dephasing in Liquids, Advances in Multi-photon Processes and Spectroscopy, Vol. 11 (World Scientific, Singapore, 1997), in press.
[7] T. Steffen, K. Duppen, Phys. Rev. Lett. 76 (1996) 1224.
[8] T. Steffen, K. Duppen, J. Chem. Phys. 106 (1997) 3854.
[9] A. Tokmakoff, G.R. Fleming, J. Chem. Phys. 106 (1997) 2569.
[10] A. Tokmakoff, M.J. Lang, D.S. Larsen, G.R. Fleming, Chem. Phys. Lett., in press.
[11] A. Tokmakoff, private communication; A. Tokmakoff, M.J. Lang, D.S. Larsen, G.R. Fleming, V. Chernyak, S. Mukamel, Two-dimensional Raman Spectroscopy of Vibrational Interactions in Liquids, Phys. Rev. Lett., submitted.
[12] S.P. Palese, J.T. Buontempo, L. Schilling, W.T. Lotshaw, Y. Tanimura, S. Mukamel, R.J.D. Miller, J. Phys. Chem. 98 (1994) 12466.
[13] J.A. Leegwater, S. Mukamel, J. Chem. Phys. 102 (1995) 2365.
[14] V. Khidekel, S. Mukamel, Chem. Phys. Lett. 240 (1995) 304; 263 (1996) 350.
[15] V. Khidekel, V. Chernyak, S. Mukamel, J. Chem. Phys. 105 (1996) 8543.
[16] A. Tokmakoff, J. Chem. Phys. 105 (1996) 13.
[17] T. Steffen, J.T. Fourkas, K. Duppen, J. Chem. Phys. 105 (1996) 7364.
[18] S. Saito, I. Ohmine, in preparation.
[19] S. Mukamel, Principles of Nonlinear Optical spectroscopy (Oxford University Press, New York, 1995).
[20] K. Okumura, Y. Tanimura, J. Chem. Phys. 107 (1997) 2267.
[21] H. Grabert, P. Schramm, G.-L. Ingold, Phys. Rep. 168 (1988) 115.
[22] K. Okumura, Y. Tanimura, Phys. Rev. E, in press.
[23] K. Okumura, Y. Tanimura, Phys. Rev. E 53 (1996) 214.
[24] K. Okumura, Y. Tanimura, J. Chem. Phys. 105 (1996) 7294.
[25] K. Okumura, Y. Tanimura, J. Chem. Phys. 106 (1997) 1687.
[26] K. Okumura, Y. Tanimura, Chem. Phys. Lett., accepted.
[27] M. Cho, M. Du, N.F. Scherer, G. Fleming, S. Mukamel, J. Chem. Phys. 99 (1993) 2410.